Photon statistical properties of photon-added two-mode squeezed coherent states*

Xu Xue-Fen(许雪芬)[a], Wang Shuai(王 帅)[b]†, and Tang Bin(唐 斌)[b]

[a] Department of Basic Course, Wuxi Institute of Technology, Wuxi 214121, China
[b] School of Mathematics and Physics, Changzhou University, Changzhou 213164, China

(Received 26 March 2013; revised manuscript received 3 June 2013; published online 20 December 2013)

We investigate photon statistical properties of the multiple-photon-added two-mode squeezed coherent states (PA-TMSCS). We find that the photon statistical properties are sensitive to the compound phase involved in the TMSCS. Our numerical analyses show that the photon addition can enhance the cross-correlation and anti-bunching effects of the PA-TMSCS. Compared with that of the TMSCS, the photon number distribution of the PA-TMSCS is modulated by a factor that is a monotonically increasing function of the numbers of adding photons to each mode; further, that the photon addition essentially shifts the photon number distribution.

Keywords: photon statistical properties, two-mode squeezed coherent state, non-Gaussian operation, photon addition

PACS: 42.50.Dv **DOI:** 10.1088/1674-1056/23/2/024206

1. Introduction

The photon-number distribution (PND) provides fundamental information on the nature of any optical field.[1] The PND for various single- and two-mode Gaussian states of an optical field, such as single-mode squeezed states and two-mode squeezed states, have been studied.[2–15] Schleich first studied photon-number oscillations in PND of squeezed coherent states and interpreted as an interference effect in phase space.[2–4] Selvadoray *et al.*[14] further studied the PND of the two-mode squeezed coherent states (TMSCS) with complex squeezing and displacement parameters by the $SU(2)$ dynamical symmetry underlying two-mode systems, and showed that the PND of the TMSCS is a periodic function of compound phase $\phi_1+\phi_2-\theta$ involved in complex squeezing and displacement parameters with a period of 2π.

In recent years, photon addition and photon subtraction represent very important experimental tools for the generation of highly nonclassical non-Gaussian quantum states; a detailed investigation of the properties of such states is certainly desirable.[16–25] The photon subtraction and addition have been realized in experiments.[26–28] For a review about quantum-state engineering by photon subtraction and addition, the readers can refer to Refs. [16] and [29] (and the references therein). For such non-Gaussian squeezed states, the PND of photon-subtracted two-mode squeezed vacuum states and photon-subtracted two-mode squeezed thermal ones have been derived.[30–32] Wang *et al.*[33] introduced the photon-added TMSCS, which is generated by adding photons to one mode of the TMSCS, and studied the nonclassical properties of the resulting states. Very recently, we have studied the photon statistical properties of photon-subtracted TMSCS,[34] as well as photon-added/photon-subtracted displaced squeezed thermal states.[35] Different from the work in Ref. [33], in this work, we consider the photon-added TMSCS (PA-TMSCS) generated by adding different photons to each mode of the TMSCS. We shall theoretically study their photon statistical properties.

This paper is organized as follows. In Section 2, we introduce the PA-TMSCS by simultaneously adding different photons to each mode of the TMSCS. With the help of the normal ordered form of the density operator of the TMSCS, we obtain its normalization constant. In Section 3, we explore the cross-correlation function and anti-bunching effect of the PA-TMSCS. In Section 4, we derive the PND of the PA-TMSCS. We find that there is a very simple yet important relationship between the PND of Gaussian TMSCS and that of the resulting non-Gaussian state. Our main results are summarized in Section 5.

2. PA-TMSCS and its normalization constant

Let us first provide a brief review of the TMSCS. The general TMSCS is generated performing the two-mode squeezing operator on an initial two-mode vacuum state first and followed by the two-mode displacement operator, i.e.

$$|\xi,\lambda_1,\lambda_2\rangle = D(\lambda_1,\lambda_2)S_2(\xi)|0,0\rangle, \tag{1}$$

*Project supported by the National Natural Science Foundation of China (Grant Nos. 11174114 and 61107055) and the Natural Science Foundation of Wuxi Institute of Technology of China (Grant No. 401301293).

†Corresponding author. E-mail: wangshuai197903@sohu.com

© 2014 Chinese Physical Society and IOP Publishing Ltd

where $S_2(\xi)$ and $D(\lambda_1,\lambda_2)$ are the two-mode squeezing and displacement operators defined by

$$\begin{aligned} S_2(\xi) &= \exp\left[\xi a^\dagger b^\dagger - \xi^* ab\right], \\ D(\lambda_1,\lambda_2) &= \exp\left[\lambda_1 a^\dagger - \lambda_1^* a + \lambda_2 b^\dagger - \lambda_2^* b\right], \end{aligned} \tag{2}$$

where $a^\dagger$ and $b^\dagger$ (a and b) are the photon creation (annihilation) operators in each mode, while

$$\xi = r\exp[\mathrm{i}\theta], \quad \lambda_1 = |\lambda_1|\exp[\mathrm{i}\phi_1], \quad \lambda_2 = |\lambda_2|\exp[\mathrm{i}\phi_2] \tag{3}$$

are complex parameters. The interchanging of the operators $D(\lambda_1,\lambda_2)$ and $S_2(\xi)$ in Eq. (1) leads to another definition of the TMSCS; both definitions are equivalent. Following the work of Ref. [13], we can re-derive the explicit representation of the TMSCS in two-mode Fock space by normal ordering techniques, i.e.,

$$\begin{aligned} |\xi,\lambda_1,\lambda_2\rangle &= \frac{1}{\cosh r}\exp\left[-\frac{1}{2}\left(\lambda_1^*\mu_1+\lambda_2^*\mu_2\right)\right. \\ &\quad \left. + a^\dagger\mu_1 + b^\dagger\mu_2 + a^\dagger b^\dagger \mathrm{e}^{\mathrm{i}\theta}\tanh r\right]|0,0\rangle, \end{aligned} \tag{4}$$

where

$$\begin{aligned} \mu_1 &= \lambda_1 - \lambda_2^* \mathrm{e}^{\mathrm{i}\theta}\tanh r, \\ \mu_2 &= \lambda_2 - \lambda_1^* \mathrm{e}^{\mathrm{i}\theta}\tanh r. \end{aligned} \tag{5}$$

Using the operator identity $: \exp[-a^\dagger a - b^\dagger b] : = |0,0\rangle\langle 0,0|$, where $: \; :$ denotes the normal ordering of annihilation and creation operators, from Eq. (1) we further obtain the normally ordered form of the density operator of the TMSCS

$$\begin{aligned} \rho &= \frac{1}{\cosh^2 r} : \exp\left[\left(a^\dagger - \lambda_1^*\right)\left(b^\dagger - \lambda_2^*\right)\mathrm{e}^{\mathrm{i}\theta}\tanh r\right. \\ &\quad + (a-\lambda_1)(b-\lambda_2)\,\mathrm{e}^{-\mathrm{i}\theta}\tanh r \\ &\quad \left. - \left(a^\dagger - \lambda_1^*\right)(a-\lambda_1) - \left(b^\dagger - \lambda_2^*\right)(b-\lambda_2)\right] : . \end{aligned} \tag{6}$$

The two expressions of the TMSCS in Eqs. (4) and (6) are useful in the following work.

We now turn to the PA-TMSCS. Theoretically, the PA-TMSCS can be obtained by repeatedly operating the photon creation operators $a^\dagger$ and $b^\dagger$ on a TMSCS

$$|\xi\rangle_{\mathrm{pa}} = C_{m,n}^{-1/2} a^{\dagger m} b^{\dagger n} |\xi,\lambda_1,\lambda_2\rangle, \tag{7}$$

where m and n are the numbers of adding photons to each mode of the TMSCS, respectively, and C is the normalization constant

$$C_{m,n} = \mathrm{Tr}\left(a^{\dagger m} b^{\dagger n} |\xi\rangle\langle\xi| a^m b^n\right). \tag{8}$$

Substituting Eq. (6) into Eq. (8) and inserting the completeness relation of two-mode coherent states, as well as using the integral formulae

$$\int \frac{\mathrm{d}^2 z}{\pi}\exp\left(\zeta|z|^2 + \xi z + \eta z^*\right) = -\frac{1}{\zeta}\exp\left[-\frac{\xi\eta}{\zeta}\right], \tag{9}$$

whose convergent condition is $\mathrm{Re}(\zeta) < 0$, after doing the straightforward calculation, we obtain

$$\begin{aligned} C_{m,n} &= \frac{\partial^{2m}\partial^{2n}}{\partial f^m \partial s^m \partial t^n \partial \tau^n}\exp\left[(fs + t\tau)\cosh^2 r\right. \\ &\quad + \frac{1}{2}\left(ft\,\mathrm{e}^{\mathrm{i}\theta} + s\tau\,\mathrm{e}^{-\mathrm{i}\theta}\right)\sinh 2r \\ &\quad \left. + f\lambda_1 + s\lambda_1^* + t\lambda_2 + \tau\lambda_2^*\right]_{f,s,t,\tau=0}. \end{aligned} \tag{10}$$

Comparing with Eq. (21) in Ref. [34], the difference between Eqs. (10) and (21) is the first item in the exponential function. It is clear that, when $m = n = 0$, $C_{0,0} = 1$ as expected. When $m = n = 1$, we have

$$\begin{aligned} C_{1,1} &= |\lambda_1\lambda_2|^2 + \left(|\lambda_1|^2 + |\lambda_2|^2\right)\cosh^2 r \\ &\quad + |\lambda_1\lambda_2|\cos\chi\sinh 2r + \cosh^2 r\cosh 2r. \end{aligned} \tag{11}$$

Obviously, $C_{1,1}$ is a periodic function of the compound phase χ involved in the TMSCS with a period of 2π, where the phase χ is defined by

$$\chi = \phi_1 + \phi_2 - \theta. \tag{12}$$

Although there are three phases ϕ_1, ϕ_2, θ, our numerical analyses show that only when $m \neq 0$ and $n \neq 0$, as well as $|\lambda_1| \neq 0$ and $|\lambda_2| \neq 0$, are all satisfied, is $C_{m,n}$ a periodic function of the compound phase χ.

The expansion of Eq. (10) is very complex. When $m = 0$ or $n = 0$, Eq. (10) reduces to the compact forms respectively

$$\begin{aligned} C_{m,0} &= \frac{\partial^{2m}}{\partial f^m \partial s^m}\exp\left[fs\cosh^2 r + f\lambda_1 + s\lambda_1^*\right]_{f,s=0} \\ &= m!\cosh^{2m} r\,\mathrm{L}_m\left(\frac{-|\lambda_1|^2}{\cosh^2 r}\right), \end{aligned} \tag{13}$$

and

$$\begin{aligned} C_{0,n} &= \frac{\partial^{2n}}{\partial t^n \partial \tau^n}\exp\left[t\tau\cosh^2 r + t\lambda_2 + \tau\lambda_2^*\right]_{t,\tau=0} \\ &= n!\cosh^{2n} r\,\mathrm{L}_n\left(\frac{-|\lambda_2|^2}{\cosh^2 r}\right), \end{aligned} \tag{14}$$

where we have used the generation function of the two-variable Hermite polynomials

$$\mathrm{H}_{m,n}(x,y) = \frac{\partial^{m+n}}{\partial t^m \partial t'^n}\exp\left[-tt' + tx + t'y\right]|_{t=t'=0}, \tag{15}$$

and the relation between the two-variable Hermite polynomials and the associated Laguerre polynomials

$$\mathrm{H}_{m,n}(\xi,\kappa) = \begin{cases} n!(-1)^n \xi^{m-n}\mathrm{L}_n^{m-n}(\xi\kappa), & m > n, \\ m!(-1)^m \kappa^{n-m}\mathrm{L}_m^{n-m}(\xi\kappa), & m < n. \end{cases} \tag{16}$$

Equations (13) and (14) are just those results of Ref. [33], which are not dependent on the phases involved in such states.

In addition, when $\lambda_1 = 0$ or $\lambda_2 = 0$, the corresponding normalization constant is also not dependent on the corresponding phases. When both $\lambda_1 = \lambda_2 = 0$, Eq. (10) reduces to the normalization constant of the photon-added two-mode squeezed vacuum state[31]

$$C'_{m,n} = m!n!\cosh^{2n} r P_m^{(0,n-m)}(\cosh 2r), \tag{17}$$

where without loss of generality assuming $m \leq n$.

3. Cross-correlation function and anti-bunching effect of the PA-TMSCS

In this section, based on the normalization constant, we shall discuss how the photon addition affects the nonclassical photon statistical properties of the PA-TMSCS in terms of the cross-correlation function and anti-bunching effect. Especially, we shall present how the compound phase χ affects those nonclassical properties.

3.1. Cross-correlation function

The cross-correlation between the two modes reflects the correlation between photons in two different modes, which plays a key role in rendering many two-mode radiations nonclassicality. The normalized cross-correlation function is defined as[36–38]

$$g_{ab}^{(2)} = \frac{\langle a^\dagger a b^\dagger b\rangle}{\langle a^\dagger a\rangle \langle b^\dagger b\rangle} - 1. \tag{18}$$

The positivity of the cross-correlation function $g_{ab}^{(2)}$ refers to correlations between two modes. By the same approach as deriving Eq. (10), we can easily calculate the average photon number of each mode of the PA-TMSCS,

$$\langle a^\dagger a\rangle_{\rm pa} = \frac{C_{m+1,n}}{C_{m,n}} - 1, \quad \langle b^\dagger b\rangle_{\rm pa} = \frac{C_{m,n+1}}{C_{m,n}} - 1, \tag{19}$$

and

$$\langle a^\dagger a b^\dagger b\rangle_{\rm pa} = \frac{C_{m+1,n+1} - C_{m+1,n} - C_{m,n+1}}{C_{m,n}} + 1. \tag{20}$$

Then, substituting Eqs. (19) and (20) into Eq. (18), we obtain the cross-correlation function of the PA-TMSCS

$$g_{ab}^{\rm pa} = \frac{C_{m,n}C_{m+1,n+1} - C_{m+1,n}C_{m,n+1}}{(C_{m+1,n} - C_{m,n})(C_{m,n+1} - C_{m,n})}. \tag{21}$$

In the range $[0, 2\pi]$, we present how the photon addition and the phase χ affect the degree of the cross-correlation of the PA-TMSCS in the case of equal displacements $|\lambda_1| = |\lambda_2|$ in Figs. 1 and 2. We can see that the photon addition weakens this cross-correlation in general. However, at certain ranges of the phase χ and squeezing parameter r, the photon addition can enhance the cross-correlation for large absolute displacements. In Fig. 2, the graph of $g_{ab}^{\rm pa}$ as a function of the squeezing parameter r for various values of (m,n) and the phase χ is presented. Comparing with Figs. 1 and 2 in our previous work,[34] we can see that both photon addition and photon subtraction can weaken or enhance the cross-correlation. For large squeezing, the influence of photon addition and photon subtraction on the cross-correlations of resulting states are almost the same.

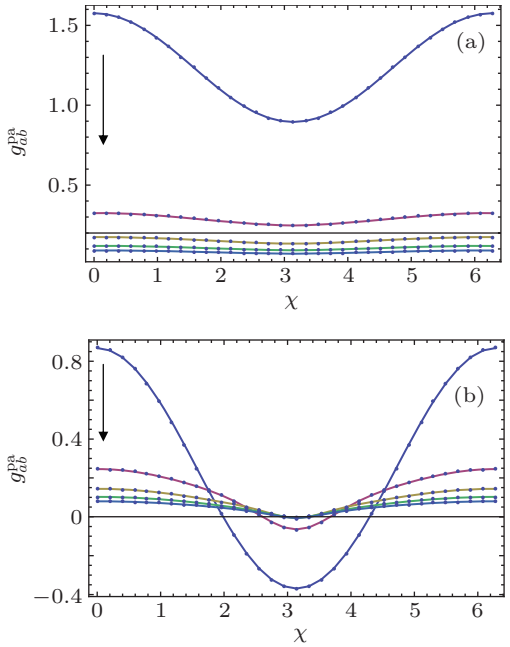


Fig. 1. (color online) The cross-correlation function as a function of the compound phase χ for different values of parameters $(|\lambda_1|, |\lambda_2|)$ and (m,n) for (a) $r = 1.0$, $|\lambda_1| = |\lambda_2| = 0.5$; (b) $r = 1.0$, $|\lambda_1| = |\lambda 2| = 1.5$. From top to bottom lines $m = n = 0, 1, 2, 3, 4$.

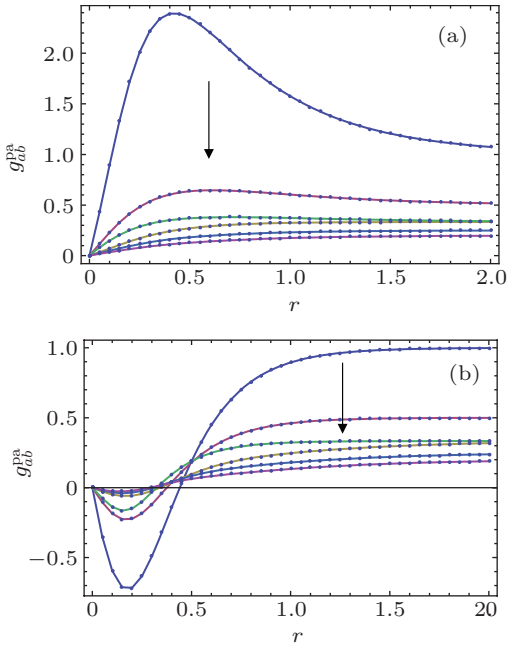


Fig. 2. (color online) The cross-correlation function as a function of the squeezing parameter r with given $|\lambda_1| = |\lambda_2| = 0.5$ for different values of χ and (m,n): (a) $\chi = 0$; (b) $\chi = \pi$. From top to bottom lines $(0,0)$, $(1,0)$, $(2,0)$, $(1,1)$, $(2,1)$, and $(2,2)$.

Our numerical analysis shows that the photon addition can weaken or enhance the cross-correlation, which is determined by the possible combinations of several parameters, i.e., the numbers of adding photons to each mode, the squeezing and absolute displacements, and the phase χ. In addition, similar to the TMSCS, $g_{ab}^{\rm pa}$ increases with the squeezing parameter r and tends to steady value for high squeezing.

3.2. Anti-bunching effect

The anti-bunching effect of the two-mode squeezed state is a nonclassical effect. Lee[39] studied the anti-bunching effects of the TMSCS. We have investigated how the photon subtraction affects the anti-bunching effect of the PS-TMSCS.[34] Here, we turn to the PA-TMSCS. The criterion for the existence of the anti-bunching effects in two-mode radiation fields is given by[39]

$$R_{ab} = \frac{\langle a^{\dagger 2}a^2\rangle + \langle b^{\dagger 2}b^2\rangle}{2\langle a^\dagger a b^\dagger b\rangle} - 1 < 0. \tag{22}$$

For the PA-TMSCS, in a similar way to Eq. (19), we have

$$\begin{aligned}\langle a^{\dagger 2}a^2\rangle_{\rm pa} &= \frac{C_{m+2,n} - 4C_{m+1,n}}{C_{m,n}} + 2,\\ \langle b^{\dagger 2}b^2\rangle_{\rm pa} &= \frac{C_{m,n+2} - 4C_{m,n+1}}{C_{m,n}} + 2.\end{aligned} \tag{23}$$

Thus, we have

$$R_{ab}^{\rm pa} = \frac{C_{m+2,n} + C_{m,n+2} + 2(\Omega - C_{m+1,n+1})}{2(C_{m+1,n+1} + \Omega)}, \tag{24}$$

$$(\Omega = C_{m,n} - C_{m+1,n} - C_{m,n+1}). \tag{25}$$

Based on Eq. (24), we can investigate how the photon addition affects the anti-bunching effects of the PA-TMSCS. The $R_{ab}^{\rm pa}$ parameter of the PA-TMSCS is a periodic function of the phase χ as shown in Fig. 3.

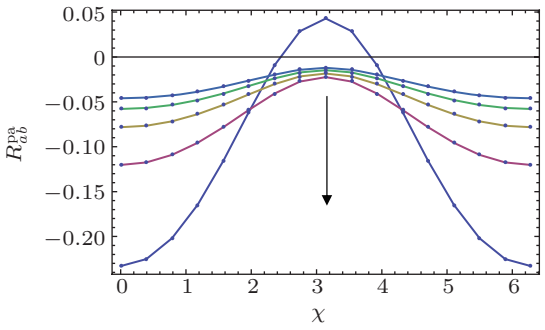


Fig. 3. (color online) The $R_{ab}^{\rm pa}$ parameter as a function of the compound phase χ with given $r = 1.0$, $|\lambda_1| = |\lambda_2| = 0.5$. From top to bottom lines $m = n = 0, 4, 3, 2, 1$.

In Fig. 4, the $R_{ab}^{\rm pa}$ as a function of the squeezing parameter is shown for different (m,n) with given $|\lambda_1| = |\lambda_2| = 0.5$. Comparing with the TMSCS, we can see that the photon addition can enhance the degree of the anti-bunching effects of the PA-TMSCS, as shown in Figs. 3, 4(a), and 4(b), especially when $\chi \to \pi$. In the case of unequal m and n, for example $n = 0$, the photon addition always weakens the degree of the anti-bunching effects, as shown in Fig. 4(c). For the case of unequal absolute displacements, we plot the $R_{ab}^{\rm pa}$ for different (m,n) in Fig. 5, which shows that the negative regions are symmetrical along the diagonal $|\lambda_1| = |\lambda_2|$. Comparing with the TMSCS and the PS-TMSCS, the negative regions of the PA-TMSCS are larger than those of the TMSCS and PS-TMSCS, and increase with the number of photon addition. In addition, for photon-added two-mode coherent states, its PND will show the anti-bunching effects.

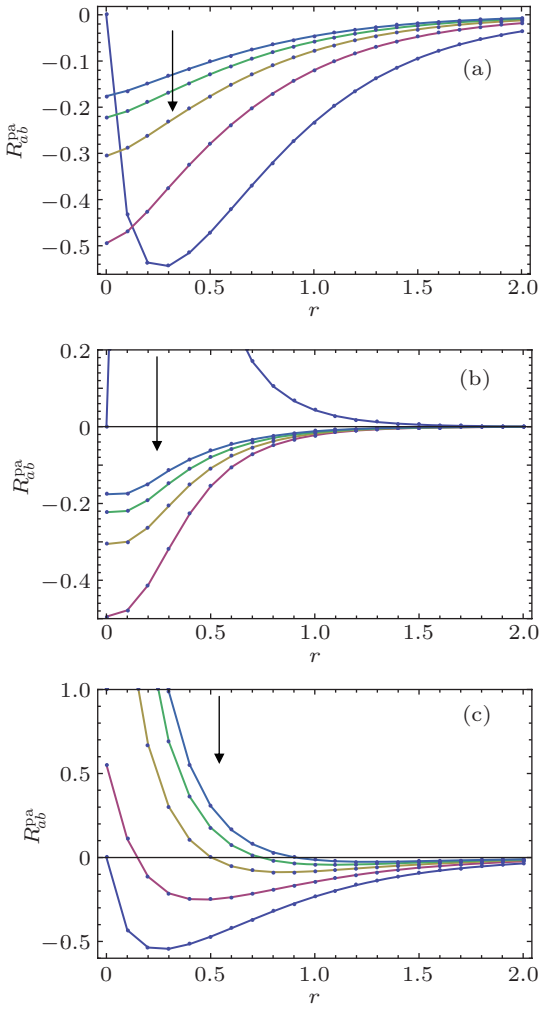


Fig. 4. (color online) The $R_{ab}^{\rm pa}$ parameter as a function of r for different values of (m,n) and the phase χ with given $|\lambda_1| = |\lambda_2| = 0.5$. (a) $\chi = 0.0$, from top to bottom lines (4,4), (3,3), (2,2), (1,1), and (0,0); (b) $\chi = \pi$, from top to bottom lines (0,0), (4,4), (3,3), (2,2), (1,1); (c) $\chi = 0$, from top to bottom lines (4,0), (3,0), (2,0), (1,0), and (0,0).

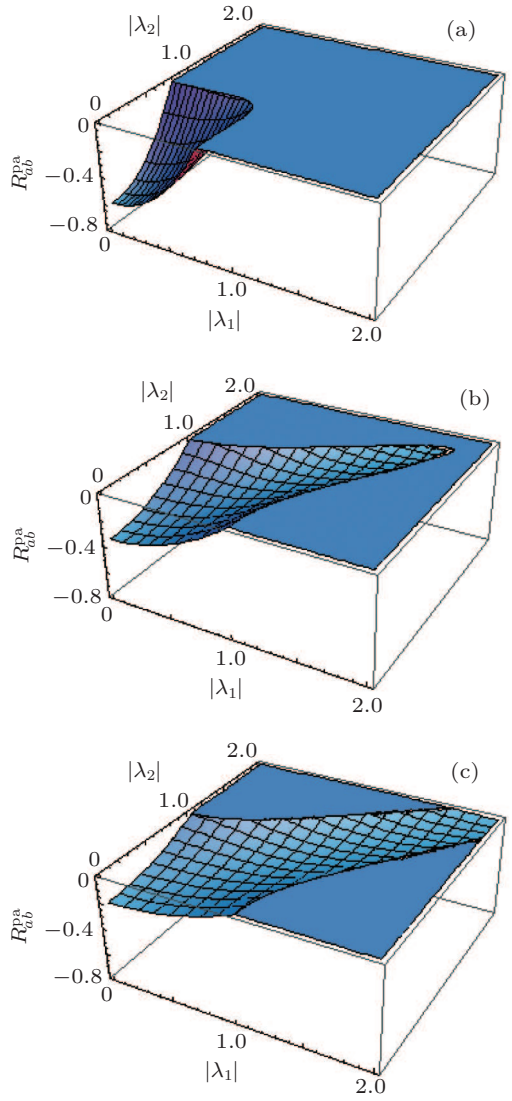


Fig. 5. (color online) The $R_{ab}^{\rm pa}$ parameter of the PA-TMSCS with given $\tanh r = 0.5$, $\chi = \pi/2$ for (a) $m = n = 0$, (b) $m = n = 1$, and (c) $m = n = 2$. The positive parts are clipped off to reveal more clearly the negative region where the nonclassical properties exist.

4. PND of the PA-TMSCS

The PND is a powerful tool with which to acquire the determination of the quantum statistical properties of the radiation field. Its oscillations are considered as a qualitative signature of nonclassicality and this type of oscillation in the PND can be explained in terms of the phase-space interference effects.[2–4] Thus, it is necessary to study the PND of the PA-TMSCS.

For the PND of the TMSCS, we can obtain it in several steps. Considered the two-variable Hermite polynomials

$$\sum_{m,n}^{\infty} \frac{t^m t'^n}{m!n!} \mathrm{H}_{m,n}(\xi,\eta) = \exp[-tt' + t\xi + t'\eta], \tag{26}$$

and Eq. (16), equation (4) can be expanded as a superposition of two-mode Fock states, i.e.

$$|\xi,\lambda_1,\lambda_2\rangle = \exp\left[-\frac{1}{2}(\lambda_1^*\mu_1 + \lambda_2^*\mu_2)\right] \times \sum_{n_a,n_b}^{\infty} \frac{(\mathrm{e}^{\mathrm{i}\theta}\tanh r)^p}{\cosh r} \left(\frac{p!}{q!}\right)^{1/2} \mu_1^{n_a-p}\mu_2^{n_b-p} \times \mathrm{L}_p^{q-p}\left(\frac{\mu_1\mu_2}{-\mathrm{e}^{\mathrm{i}\theta}\tanh r}\right)|n_a,n_b\rangle, \tag{27}$$

where

$$p \equiv \min(n_a,n_b), \quad q \equiv \max(n_a,n_b), \tag{28}$$

which is just the result of Ref. [13] with real squeezing parameter. Based on Eq. (27), we can easily obtain the PND of the TMSCS

$$P_0(n_a,n_b) = \exp\left[-\frac{1}{2}(\lambda_1^*\mu_1 + \lambda_1\mu_1^*) - \frac{1}{2}(\lambda_2^*\mu_2 + \lambda_2\mu_2^*)\right] \times \frac{(\tanh r)^{2p}}{\cosh^2 r}\frac{p!}{q!}|\mu_1|^{2(n_a-p)}|\mu_2|^{2(n_b-p)} \times \left|\mathrm{L}_p^{q-p}\left(\frac{\mu_1\mu_2}{-\mathrm{e}^{\mathrm{i}\theta}\tanh r}\right)\right|^2. \tag{29}$$

Substituting Eq. (5) into Eq. (29), one can easily prove that the PND of the TMSCS is a periodic function of compound phase χ with a period of 2π. Selvadoray *et al.*[14] had studied the dependence of the PND of the TMSCS on the phase χ in great detail.

Now we turn to the PND of the PA-TMSCS. The joint probability to find n_a photons in mode a and n_b photons in mode b, i.e., the photon-number distribution $P_{\rm pa}(n_a,n_b)$ is given by

$$P_{\rm pa}(n_a,n_b) = \left|\langle n_a,n_b|C_{m,n}^{-1}a^{\dagger m}b^{\dagger n}|\xi,\lambda_1,\lambda_2\rangle\right|^2, \tag{30}$$

where $|n_a,n_b\rangle$ are the two-mode Fock states. Thus, the PND of the PA-TMSCS can be easily obtained

$$P_{\rm pa}(n_a,n_b) = \frac{C_{m,n}^{-1}n_a!n_b!}{(n_a-m)!(n_b-n)!}P_0(n_a-m,n_b-n). \tag{31}$$

Equation (31) shows that there is no photon distribution when $n_1 < m$ or $n_2 < n$, respectively, which is different from that of the PS-TMSCS. Compared wtih the PND of the TMSCS, equation (31) indicates that the PND of the PA-TMSCS is modulated by a factor that is a monotonically increasing function of m and n. We plot the variations of the PND of the PA-TMSCS with respect to (m,n) and the compound phase χ in Fig. 6.

We can see from Fig. 6 that when $|\lambda_1| = |\lambda_2|$ and $m = n$, the PND is symmetrical along the diagonal line of $n_a = n_b$. By adding photons to the TMSCS, we can move the peak of the PND from zero photons to nonzero photons. This is clearly seen in Fig. 6. The reason why the peak moves to a higher

photon number is because of the coefficient of the creation operation

$$a^{\dagger}|n\rangle = \sqrt{n+1}\,|n+1\rangle\,.$$

This coefficient gives a higher weight to the initial higher-number photon component. In addition, the shape of $P_{\rm pa}(n_a,n_b)$ becomes more flat and wide than that of the TMSCS. Obviously, the PND of the PA-TMSCS is very sensitive to the phase χ. When χ approaches to π, the PND in each mode of the PA-TMSCS shows giant oscillations especially for large squeezing, which may be explained by the concept of interference in phase space.[2–4]

Our numerical analysis shows that when the number of adding photons to mode a is larger than that from mode b, i.e. $m > n$, the peaks of the PND are shifted to the n_a axis. In the case of unequal absolute displacements, for example, when $|\lambda_1| > |\lambda_2|$, the peaks of the PND are shifted to the n_a axis. Therefore, the properties of the PND not only depend on how much the state is squeezed and displaced initially, but also on how many photons are added to each mode.

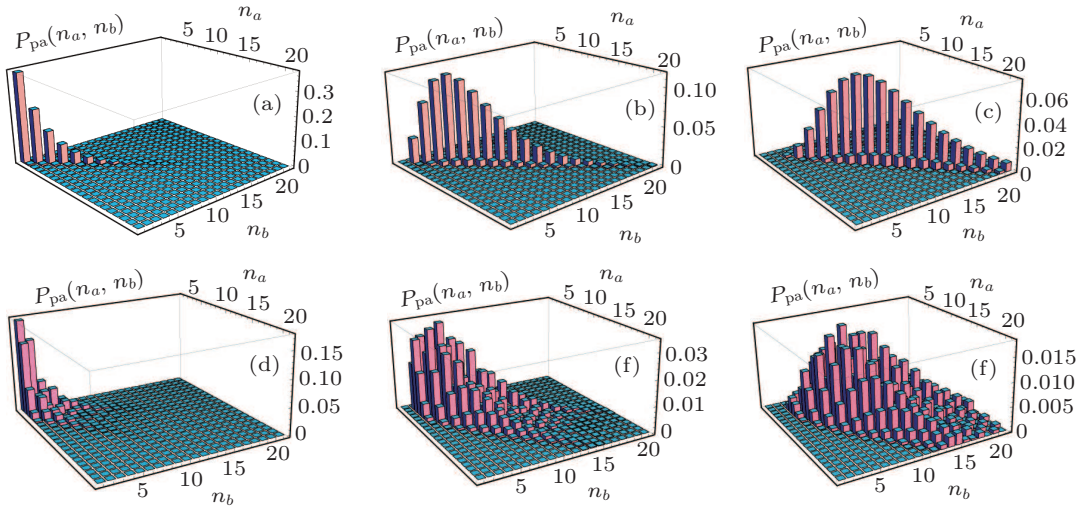


Fig. 6. (color online) Photon-number distributions of the PA-TMSCS with $r = 1.0$ and $|\lambda_1| = |\lambda_2| = 0.5$, for $\chi = 0$: (a) $m = n = 0$, (b) $m = n = 1$, (c) $m = n = 2$, and for $\chi = \pi$: (d) $m = n = 0$, (e) $m = n = 1$, (f) $m = n = 2$.

5. Conclusions

In conclusion, we have investigated how the photon addition affects the photon statistical properties of the PA-TMSCS based on the cross-correlation function, anti-bunching effects and its PND. We find that, similar to that of the PS-TMSCS, the normalization constant, the cross-correlation function, the criterion of the anti-bunching effects and the PND of the PA-TMSCS are all periodic functions of the compound phase χ with a period of 2π. When $\lambda_1 = 0$ or $\lambda_2 = 0$, these quantities are all phase-independent. Our numerical analysis shows that the photon addition can enhance the cross-correlation and anti-bunching effects for appropriate combinations of several parameters involved in the PA-TMSCS. Compared with that of the TMSCS, the PND of the PA-TMSCS is modulated by a factor that is a monotonically increasing function of photon addition numbers m and n. The photon addition essentially shifts the PND. There is no photon distribution when $n_1 < m$ or $n_2 < n$, respectively, which is different from that of the PS-TMSCS.

References

[1] Mandel L and Wolf E 1995 *Optical Coherence and Quantum Optics* (Cambridge: Cambridge University Press)
[2] Schleich W, Walls D F and Wheeler J A 1988 *Phys. Rev. A* **38** 1177
[3] Schleich W and Wheeler J A 1987 *Nature* **326** 574
[4] Schleich W and Wheeler J A 1987 *J. Opt. Soc. Am. B* **4** 1715
[5] Agarwal G S and Adam G 1988 *Phys. Rev. A* **38** 750
[6] Agarwal G S and Adam G 1989 *Phys. Rev. A* **39** 6259
[7] Chaturvedi S and Srinivasan V 1989 *Phys. Rev. A* **40** 6095
[8] Kim M S, de Oliveira F A M and Knight P L 1989 *Phys. Rev. A* **40** 2494
[9] Peřina J and Bajer J 1990 *Phys. Rev. A* **41** 516
[10] Dutta B, Mukunda N, Simon R and Subramaniam A 1993 *J. Opt. Soc. Am. B* **10** 253
[11] Dodonov V V, Man'ko O V and Manko V I 1994 *Phys. Rev. A* **49** 2993
[12] Lee C T 1990 *Phys. Rev. A* **42** 4193
[13] Caves C M, Zhu C, Milburn G J and Schleich W 1991 *Phys. Rev. A* **43** 3854
[14] Selvadoray M, Kumar M S and Simon R 1994 *Phys. Rev. A* **49** 4957
[15] Wang S, Zhang X Y and Fan H Y 2012 *Chin. Phys. B* **21** 054206
[16] Dell's Anno F, De Siena S and Illuminati F 2006 *Phys. Rep.* **428** 53
[17] Wenger J, Tualle-Brouri R and Grangier P 2004 *Phys. Rev. Lett.* **92** 153601

[18] Nha H and Carmichael H J 2004 *Phys. Rev. Lett.* **93** 020401
[19] García-Patrón R, Fiurášek J, Cerf N J, Wenger J, Tualle-Brouri R and Grangier Ph 2004 *Phys. Rev. Lett.* **93** 130409
[20] Takahashi H, Neergaard-Nielsenl J S, Takeuchil M, Takeokal M, Hayasakal K, Furusawa A and Sasakil M 2010 *Nat. Photon.* **4** 178
[21] Agarwal G S and Tara K 1991 *Phys. Rev. A* **43** 492
[22] Hu L Y and Fan H Y 2009 *Chin. Phys. B* **18** 4657
[23] Zhou J, Fan H Y and Song J 2012 *Chin. Phys. B* **21** 070301
[24] Xu L J, Tan G B, Ma S J and Guo Q 2013 *Chin. Phys. B* **22** 030311
[25] Wang S, Yuan H C and Xu X F 2013 *Eur. Phys. J. D* **67** 102
[26] Ourjoumtsev A, Tualle-Brouri R, Laurat J and Grangier Ph 2006 *Science* **312** 83
[27] Boyd R W, Chan K W and O'Sullivan M N 2007 *Science* **317** 1874
[28] Zavatta A, Parigi V, Kim M S, Jeong H and Bellini M 2009 *Phys. Rev. Lett.* **103** 140406
[29] Kim M S 2008 *J. Phys. B: At. Mol. Opt. Phys.* **41** 133001
[30] Zhang Z X and Fan H Y 1993 *Phys. Lett. A* **174** 206
[31] Hu L Y, Jia F and Zhang Z M 2012 *J. Opt. Soc. Am. B* **29** 1456
[32] Meng X G, Wang Z, Fan H Y, Wang J S and Yang Z S 2012 *J. Opt. Soc. Am. B* **29** 1844
[33] Wang X B, Kwek L C, Liu Y and Oh C H 2001 *J. Phys. B: At. Mol. Opt. Phys.* **34** 1059
[34] Wang S, Yuan H C and Xu X F 2013 *Opt. Commun.* **298–299** 154
[35] Wang S, Fan H Y and Hu L Y 2012 *J. Opt. Soc. Am. B* **29** 1020
[36] Walls D F and Milburn G J 1995 *Quantum Optics* (Berlin: Springer-Verlag)
[37] Lai W K, Buzek V and Knight P L 1991 *Phys. Rev. A* **44** 6043
[38] Zhang W M, Feng D F and Gilmore R 1990 *Rev. Mod. Phys.* **62** 867
[39] Lee C T 1990 *Phys. Rev. A* **41** 1569